Neuron, Vol. 18, 59–70, January, 1997, Copyright ©1997 by Cell Press

Assembly of CNS Myelin in the Absence of Proteolipid Protein

Matthias Klugmann, Markus H. Schwab, Anja Pühlhofer, Armin Schneider, Frank Zimmermann, Ian R. Griffiths,* and Klaus-Armin Nave
Zentrum für Molekulare Biologie (ZMBH)
University of Heidelberg
D-69120 Heidelberg
Federal Republic of Germany
*Department of Veterinary Clinical Studies
University of Glasgow
United Kingdom

Summary

Two proteolipid proteins, PLP and DM20, are the major membrane components of central nervous system (CNS) myelin. Mutations of the X-linked PLP/DM20 gene cause dysmyelination in mouse and man and result in significant mortality. Here we show that mutant mice that lack expression of a targeted PLP gene fail to exhibit the known dysmyelinated phenotype. Unable to encode PLP/DM20 or PLP-related polypeptides, oligodendrocytes are still competent to myelinate CNS axons of all calibers and to assemble compacted myelin sheaths. Ultrastructurally, however, the electron-dense 'intraperiod' lines in myelin remain condensed, correlating with its reduced physical stability. This suggests that after myelin compaction, PLP forms a stabilizing membrane junction, similar to a "zipper." Dysmyelination and oligodendrocyte death emerge as an epiphenomenon of other PLP mutations and have been uncoupled in the PLP null allele from the risk of premature myelin breakdown.

Introduction

The formation of myelin sheaths by oligodendrocytes in the central nervous system (CNS) and Schwann cells in the periphery provides the cellular basis for rapid impulse conduction (Raine, 1984; Bunge and Fernandez-Valle, 1995). Naturally occuring diseases in which axons fail to be ensheathed ("dysmyelination") or loose their insulating myelin ("demyelination") have been described in mouse and man and comprise a heterogenous group of disorders associated with a characteristic impairment of motor and sensory functions (for review see Lupski et al. 1993; Snipes et al., 1993; Nave, 1995; Snipes and Suter, 1995; Nave and Boespflug-Tanguy, 1996).

The elaboration of myelin requires the large-scale synthesis of myelin-specific lipids and membrane-associated proteins (Pfeiffer et al., 1993; Campagnoni, 1995), presumed to play specific roles in spiral wrapping, membrane compaction, and the fine architecture of the multilayered myelin sheath. Two membrane-associated proteins predominate in abundance, myelin basic protein (MBP) and proteolipid protein (PLP/DM20) (Braun, 1984; Lees and Brostoff, 1984). It is widely believed that the two proteins play similar structural roles in myelin and are required for intra- and extracellular myelin compaction. For MBP, direct genetic evidence for the adhesive function came with the mouse mutant *shiverer*, a naturally occurring MBP null allele (Roach et al., 1985). *Shiverer* myelin, where present, is only thin and has no major dense line (MDL), the ultrastructural correlate of intracellular myelin compaction. Although the overall lack of CNS myelin in this mutant has not been fully explained, *shiverer* mice have established that MBP is required for intracellular membrane adhesion (Readhead et al., 1987; Martini et al., 1995). In contrast, to define PLP function with the help of mutants has yielded results that suggest more complex pathogenic mechanisms.

PLP is an integral "four-helix-span" membrane protein with a molecular mass of 30 kDa (Milner et al., 1985; Popot et al., 1991; Weimbs and Stoffel, 1992). A smaller isoform, termed DM20 (molecular mass 26.5 kDa), is derived by alternative mRNA splicing (Nave et al., 1987). DM20 is detectable early in the oligodendrocyte lineage preceding many other myelin proteins (Ikenaka et al., 1992; Timsit et al., 1995; Dickinson et al., 1996), but its function at these early stages is not known. The primary structure of PLP/DM20 is highly conserved (100% between mouse and man), which suggests that the protein engages in multiple protein–protein interactions. More recently, DM20 has been identified as the prototype of a new protein family, which also includes two neuronal proteins, M6A (EMA) and M6B (Baumrind et al., 1992; Lagenaur et al., 1992; Yan et al., 1993).

The view that PLP/DM20 and MBP play similar roles in myelin received initial strong support when naturally occurring PLP mutants were identified (Nave et al., 1986; Hudson et al., 1987). Point mutations and RNA splice defects were documented in the *jimpy* and the *jimpy*^{msd} mouse, the *myelin-deficient* rat, and later in other species, including a growing number of human patients with Pelizaeus-Merzbacher (PMD) disease and X-linked spastic paraplegia (SPG-2) (reviewed in Hodes et al., 1994; Nave and Boespflug-Tanguy, 1996; Seitelberger et al., 1996). Point mutations that alter the primary structure of PLP and DM20 render these proteins as misfolded polypeptides that are unable to exit from intracellular compartments and are rapidly degraded (Roussel et al., 1987; Gow et al., 1994; Jung et al., 1996).

In *jimpy* mice, immature oligodendrocytes are increased, and the majority of differentiated oligodendrocytes die at an early stage with morphological features of apoptosis (Knapp et al., 1986; Skoff, 1995). Less than 5% of the normal number of CNS axons are eventually ensheathed, and myelinated axons are ultrastructurally abnormal (Duncan et al., 1989). PLP-mutant mice show significant deficits of normal motor performance and, in most cases, tremors, seizures, and premature death. Some of the natural rodent mutants exert no obvious effect on oligodendrocyte survival but display a widespread dysmyelination of the CNS (Schneider et al., 1992; Tosic et al., 1994). The *rumpshaker* mutation in mice has demonstrated that this dysmyelination is not the cause of oligodendrocyte death (Schneider et al., 1992).

A further complication in understanding the PLP-linked dysmyelinating diseases was the observation that increasing the wild-type PLP gene dosage results, by itself, in a phenotype that is in many respects similar to the effect of a mutation. Only 2-fold transcriptional PLP/DM20 overexpression in transgenic mice is sufficient to turn the PLP gene into a disease gene (Readhead et al., 1994), and slightly higher overexpression rates cause abnormal oligodendrocyte death (Kagawa et al., 1994). Duplications of the human PLP gene have likewise been associated with PMD (Ellis and Malcolm, 1994; Carango et al., 1995; Inoue et al., 1996) and account for about 50% of all familial cases of this disease (Nave and Boespflug-Tanguy, 1996).

Taken together, the available genetic data have suggested that normal myelin formation is extremely sensitive to qualitative and quantitative alterations in the expression of the PLP/DM20 gene. In all known mutations, the cellular phenotypes are complex because different pathological events overlap. These are (1) the intracellular retention of misfolded PLP, (2) the dysmyelination of CNS axons, most notably the numerous 'naked' axons in white matter tracts, (3) abnormal myelin compaction, and (4) in many mutants, the premature death of oligodendrocytes with morphological features of apoptosis.

We have constructed two independent lines of transgenic mice that represent null alleles and completely lack expression of PLP, DM20, or PLP/DM20-related polypeptides. Surprisingly, none of the major pathological features previously associated with the mutations of this gene were found. Oligodendrocytes survive, are myelination competent, and recognize small and large-caliber axons. However, compacted myelin sheaths are extremely susceptible to loosen and decompact in conditions of suboptimal fixation during tissue processing. There is no equivalent evidence of in vivo myelin breakdown nor functional consequences on behavior, at least in the first year of life. At older ages, a destabilization of compacted myelin becomes more prominent and may indicate a slowly progressive myelin pathology. We have also generated double-mutant mice that lack both PLP and MBP, and which confirm that the two major myelin proteins serve very different functions in the assembly of CNS myelin.

Results

Gene Targeting and Transgenic Complementation

To create a true PLP/DM20 null allele, we constructed a gene replacement vector that eliminates, by homologous recombination, the translation start site for PLP and DM20. The 3′ part of exon 1, including the translation start codon (Ikenaka et al., 1988), and a 2.5 kb fragment of the first intron were replaced by the neomycin (neo) resistance gene as shown schematically in Figure 1A. Electroporation of mouse embryonic stem cells resulted in the generation of G418-resistant clones with a 1-in-46 frequency of correct targeting events (six clones). Homologous recombination was confirmed by Southern blot analysis (Figure 1B). A neo probe was used to verify a single integration event (not shown). Blastocyst injections of two clones yielded highly chimeric mice, which were used to establish independent transgenic lines that did not differ in phenotype. Heterozygous females (plp−/+) were bred with wild-type (plp+/Y) males to obtain hemizygous mutants (plp−/Y). In some crosses, we used males from PLP-transgenic lines (#66 and 72) transmitting an autosomal copy of the wild-type PLP gene (Readhead et al., 1994). In the progeny of the latter cross, we expected 50% hemizygous mutants, about half of which should be immediately "rescued" by transgenic complementation. All genotypes were found at the expected frequencies, and mice developed normally.

Motor Performance

In contrast to most naturally occurring PLP mutants, hemizygous males were fully viable, reproduced normally, and thus allowed the generation of homozygous females (plp−/−). Obvious signs of abnormal motor development were lacking, and tremors or seizures were absent. We performed a more specialized locomotor test of plp−/Y mice at the age of 6 months. This cohort of mice was tested again at 12 months of age to detect possible losses of motor performance. The 'rotarod test' (Figure 2) failed to reveal any performance deficit, suggesting that motor development is not compromised in the absence of PLP and DM20. The same paradigm has revealed significant motor deficits associated with dysmyelination of plp^{neo} mice (Boison et al., 1995). We could likewise show a significant motor defect of PLP-transgenic *rumpshaker* mice, which served as positive controls for this assay (the wild-type PLP-transgene improves the *rumpshaker* phenotype but does not completely rescue it; A. Schneider, I. Griffiths, and K.-A. Nave, unpublished data). There was also no behavioral abnormality of plp−/Y mice when challenged to balance on a thin horizontal bar and when tested in a standard open field setting (data not shown).

Loss of PLP/DM20 Gene Expression

By in situ hybridization, using a riboprobe complementary to exons 1–7, no PLP signal was detected in plp−/Y brain sections, in contrast to a strong hybridization in the wild type (data not shown). By Northern blot analysis of adult plp−/Y brain RNA, no PLP mRNA was detectable (Figure 1C) except for a 3.4 kb mRNA of very low abundance (see Discussion). The corresponding cDNA was cloned by reverse transcription–polymerase chain reaction (PCR) (using primers from PLP exons 1 and 3), and its nucleotide sequence was determined. This analysis revealed that intron 1 of the mutant PLP transcript was removed due to a cryptic donor splice site located in the neo gene. The 3.4 kb RNA contains no open reading frame for PLP or PLP-related peptides. The absence of PLP and DM20 in plp−/Y mice was confirmed by Western blot analysis of purified myelin preparation (Figure 1D) or total brain extracts (not shown).

Immunocytochemistry of Myelin

In white matter tracts of hemizygous males (and homozygous plp−/− females), no myelinated fibers were immunostained with an antibody against PLP/DM20,

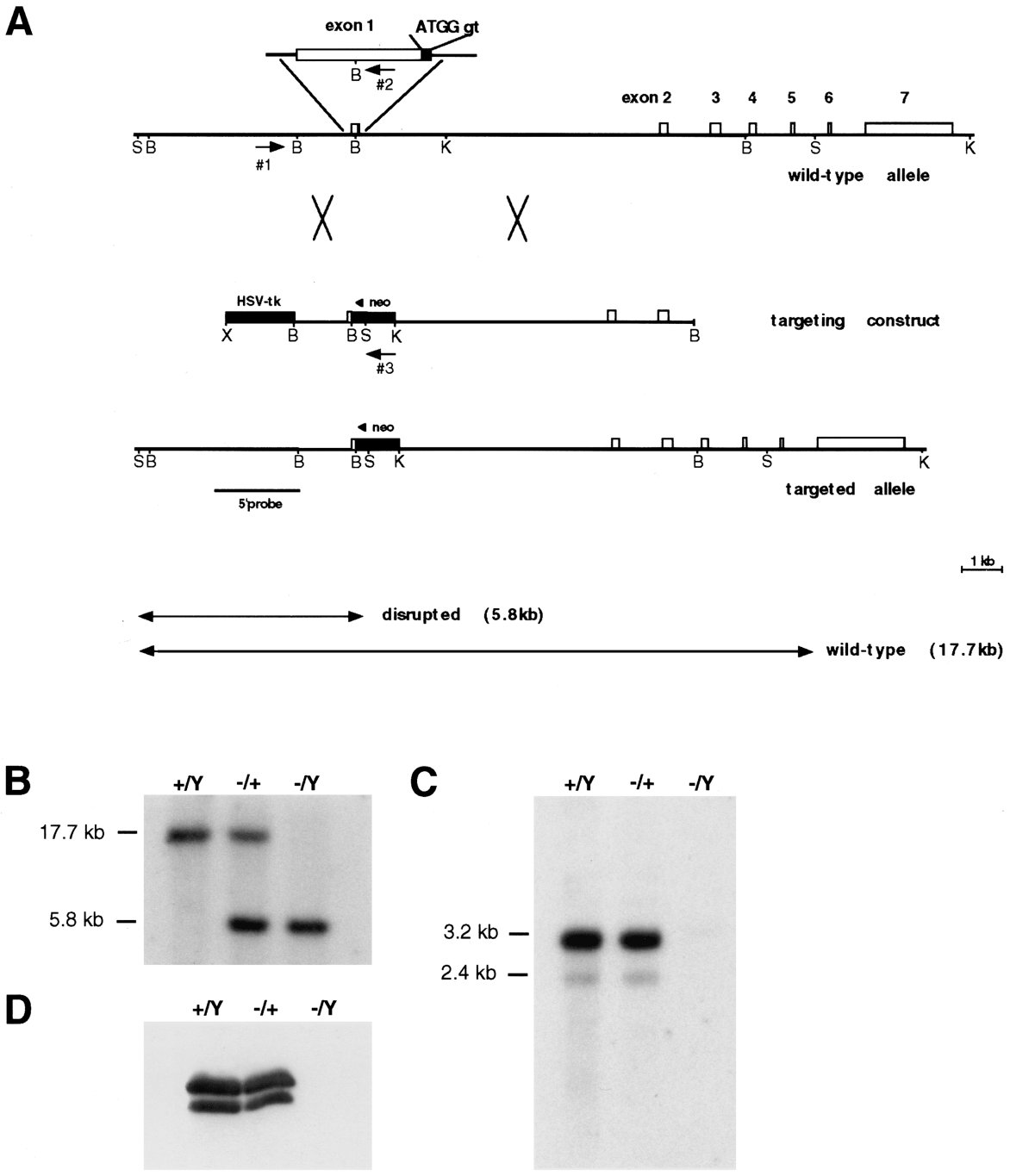

Figure 1. Targeted Inactivation of the Myelin Proteolipid Protein Gene

(A) Structure of the mouse PLP/DM20 gene (wild type), the targeting construct, and the targeted gene. The PLP/DM20 locus comprises seven exons indicated as open boxes. Note that after homologous recombination, 2.5 kb of intron 1 and the 3′ end of exon 1 are removed, which also deletes the translational initiation codon (ATG) located adjacent to the first exon–intron boundary (enlarged on top). The neomycin resistance gene (neo) is transcribed in antisense orientation relative to PLP. Positions of the 5′ probe, used for Southern analysis, and primers #1 (sB4ext), #2 (PLP5′a), and #3 (Mkneo1), used for genotyping, are indicated. Restriction sites are B (BamHI), K (KpnI), S (SphI), and X (XhoI).

(B) Southern analysis of genomic DNA from wild-type (+/Y), heterozygous (+/−), and hemizygous (−/Y) mutant mice. Correct genomic targeting introduces an additional SphI restriction site (in neo). When hybridized to the 5′ probe, SphI fragments are 17.7 kb in the wild-type and 5.8 kb in the mutant allele. When stripped and rehybridized to a neo-specific probe, a single band is obtained with DNA from heterozygous (+/−) and hemizygous (−/Y) mice but not with DNA from wild-type mice (not shown).

(C) Northern analysis of adult brain RNA (5 μg/lane). Transcription of the wild-type PLP/DM20 gene yields differentially polyadenylated mRNAs of 3.2 kb, 2.4 kb, and 1.6 kb (+/Y), also detectable in brains of heterozygous females (−/+). Gene targeting drastically reduces the steady-state level of PLP transcripts, most likely due to "antisense" transcription of neo in close proximity to the PLP promoter. A 3.4 kb RNA that lacks any PLP/DM20 coding capacity is visible on long exposures (see text).

(D) Western blot analysis. Purified CNS myelin from wild-type, heterozygous (+/−), and hemizygous (−/Y) mice (10 μg/lane) stained with a polyclonal antiserum directed against the common C-terminus of PLP and DM20. Both proteolipids are also absent when total brain extracts are analyzed (not shown).

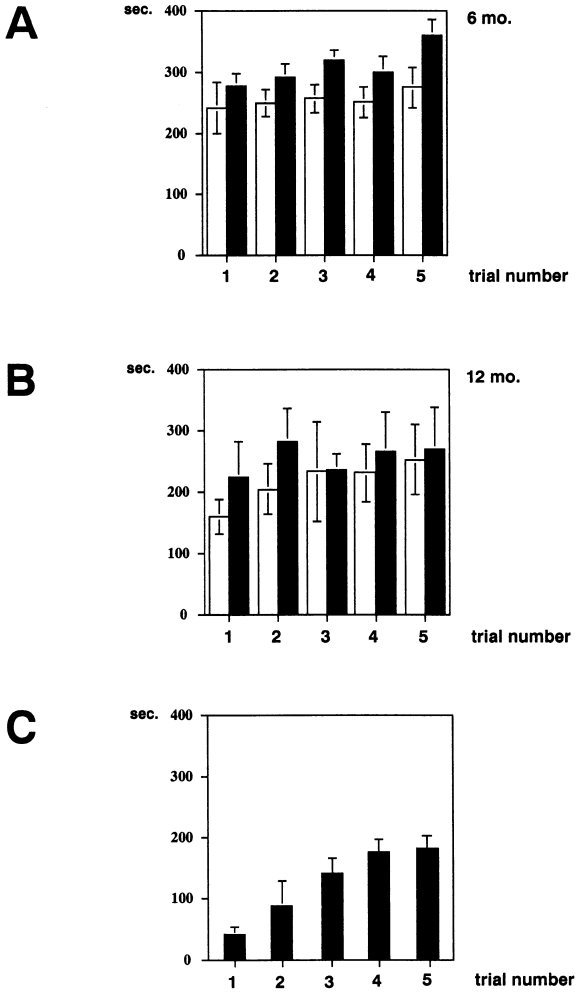

Figure 2. Motor Performance of plp^{null} Mice

(A) The 'rotarod' test was used to measure motor performance of 6-month-old plp^{null} mice (closed bars) and age-matched controls (open bars). In a series of five consecutive trials, the cumulative time (in seconds ± SEM) was scored in which animals of each genotype (n = 6) were able to stay on a slowly rotating roller. After 15 s at rest, rotating speed (starting at 1 rpm) was increased in 60 s intervals to 2, 4, 8, 12, 16, and 20 rpm. There was no detectable motor defect in the absence of PLP expression.

(B) The rotarod assay was repeated at 1 year of age, using the same cohort of mice. Whereas the overall performance was slightly decreased, the null allele was not significantly impaired.

(C) To show that the paradigm is principally adequate to reveal a mild dysmyelination, a cohort of PLP-transgenic *rumpshaker* mutants was tested under the same conditions. Note that the total time scored in this experiment was reduced compared to that of wild-type mice (A and B).

whereas MBP reactivity was strong (Figures 3A and 3B). No evidence of astrocytosis was present, as assessed by GFAP immunostaining (Figure 3C). The periaxonal localization of myelin-associated glycoprotein (MAG) was unchanged, indicating that this adhesion molecule has not redistributed and substituted for PLP within compacted myelin (Figure 3D). Random X chromosome–inactivation in females allows a direct side-by-side comparison of mutant and wild-type myelin processed under the identical conditions. The staining of spinal cord and optic nerve sections in adult heterozygotes with an anti-PLP/DM20 antibody revealed a mosaicism that varied from patches containing predominantly PLP-positive or -negative sheaths to regions of complete intermingling (Figures 3E and 3G). There was no astrocytosis associated with the patches of PLP-negative fibers (Figure 3F). The absence or presence of PLP/DM20 affected large and small diameter fibers (Figure 3G), and myelin sheaths of PLP-negative fibers were of equal thickness and well compacted when adjacent sections were stained for MBP.

Oligodendrocyte Survival

We noticed that in male F0 chimeras that were 90%–100% embryonic stem (ES) cell–derived (as estimated by the *agouty* coat color marker), only 30% of the myelin sheaths in the spinal cord were PLP-negative and thus assembled by mutant oligodendrocytes (data not shown). This suggested that PLP/DM20-negative cells could have a developmental defect. However, counts of PLP/DM20 immunoreactive sheaths in sections of the thoracic cord of F1 heterozygote females (n = 4) revealed a proportion of 57% ± 3% PLP-positive sheaths (mean ± SEM; n = 400). This number is close to the theoretical value of 50% (Tan et al., 1995) and demonstrates, at least indirectly, that PLP/DM20-deficient oligodendrocytes survive and ensheath normally in the "competitive" situation of the chimeric CNS. No evidence of increased cell death or degenerative changes were seen in PLP/DM20-deficient oligodendrocytes (not shown).

Myelin Defects at the Ultrastructural Level

Multiple regions of the CNS from plp−/Y mice, examined in 1 μm resin sections at various ages from 5 weeks to 1 year, appeared normally myelinated. This was confirmed on ultrathin sections from spinal cord of adult mice (Figure 4A). No difference was noted in the proportion of myelinated axons, myelin sheath thickness, or size range of myelinated fibers between plp−/Y and wild-type mice. This is in complete contrast to the dysmyelination seen in even the least severe of the natural plp mutants, *rumpshaker* (Figure 4B). In regions with excellent fixation (assessed by criteria such as size of extracellular space, swelling of astrocyte processes, and swelling of mitochondria), myelin of null mutants was compacted. However, the difference between MDL and intraperiod line (IPL) was less distinct than in wild type (Figures 4C and 4D), with the IPL being a single condensed structure, similar in appearance to that seen in natural mutants (Figure 4E). In a minority of regions, a double IPL was noted and could coexist with the condensed IPL in the same sheath. Where tissue perfusion was less than optimal, the sheaths were less compacted and more loose than would be expected in normal mice. The appearance of the myelin sheath remained unchanged for up to at least 1 year of age, with no evidence of myelin breakdown and no microglial or macrophage response.

We used a serial thick-and-thin sectioning procedure to identify, first by immunocytochemistry of 1 μm resin sections, individual PLP-positive and -negative fibers in the chimeric heterozygous mice, and then the adjacent

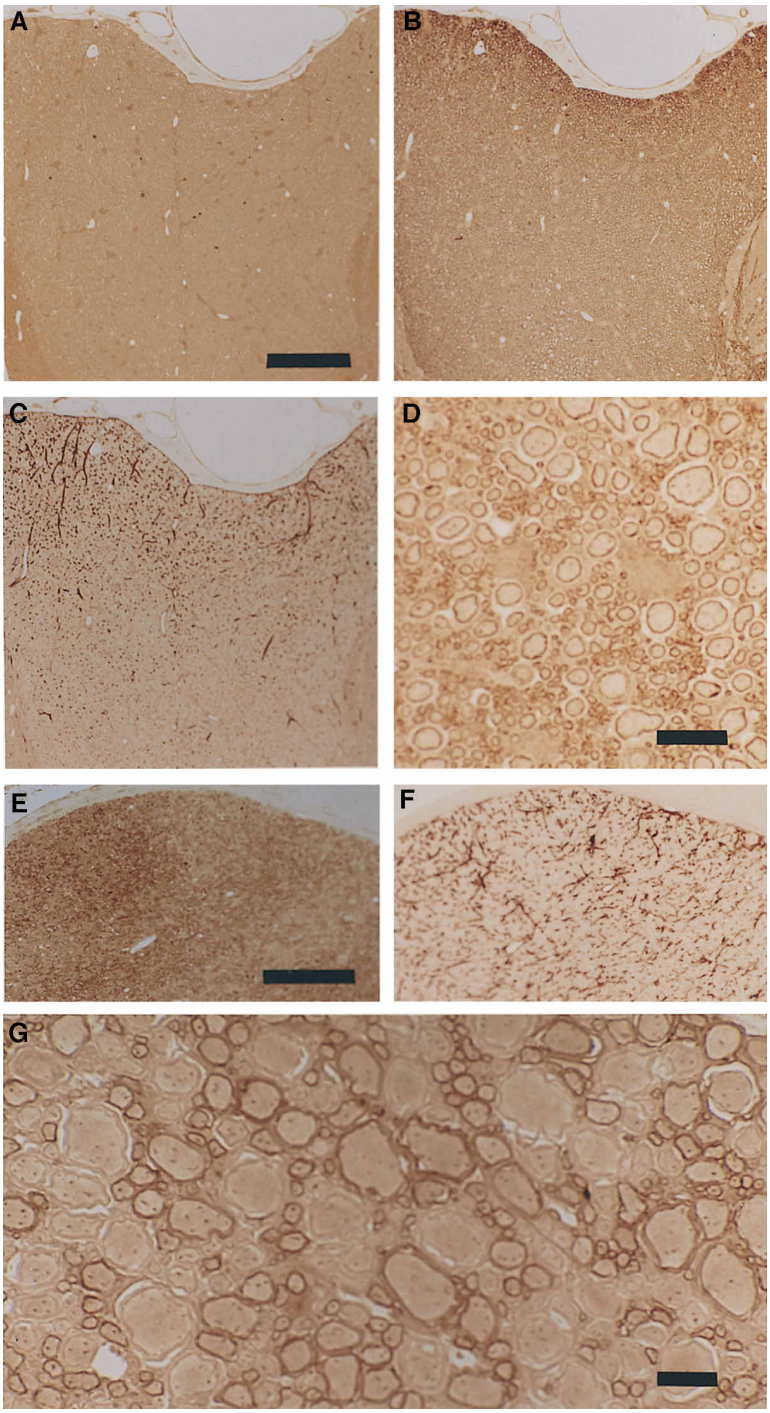

Figure 3. Immunocytochemistry of PLP-Deficient White Matter Tracts

(A–C) Immediately adjacent 1 μm resin sections of dorsal columns of cervical spinal cord from a 4-month-old plp−/Y mouse immunostained by the PAP technique for PLP (A), MBP (B), and GFAP (C). The myelin sheaths show strong staining with MBP but are negative for PLP. The distribution of GFAP-positive astrocytes is normal, showing a lack of astrocytosis. Scale bar = 100 μm.

(D) The cord from the same mouse stained for MAG, which is distributed normally in the periaxonal space. Scale bar = 10 μm.

(E and F) Immediately adjacent sections from the optic nerve of a plp−/+ heterozygote immunostained for PLP (E) and GFAP (F). The PLP staining shows patches containing predominantly PLP+ or PLP− myelin sheaths. There is no astrocytosis associated with the PLP− areas. Scale bar = 100 μm.

(G) Region of spinal cord lateral column from a plp−/+ heteozygote immunostained for PLP. A mosaic of staining is present with no selectivity of fiber size on the basis of presence or absence of PLP staining. Scale bar = 5 μm.

thin sections to determine their specific ultrastructural features by electron microscopy. The findings in PLP-negative fibers of the chimera were identical to those in plp−/Y mice, with well compacted regions of a sheath together with areas of looser appearance; the IPL was frequently condensed (Figures 4F–4H).

Compensatory Mechanisms

To investigate the possibility that other myelin proteins compensate for the lack of PLP/DM20, we analyzed purified myelin from adult plp−/Y and control mice. The overall pattern of size-separated proteins, stained with Coommassie blue (Figure 5A) or by silver impregnation (not shown), did not differ beween wild-type and mutant mice, except for the obvious lack of PLP in plp−/Y brains. No protein emerged at the abundance that would be sufficient to compensate for the lack of the two proteolipids. By Western blot analyses (Figure 5B), other known CNS myelin proteins (MBP, MAL, and OSP) were unchanged, and PNS myelin proteins tested (P0 and

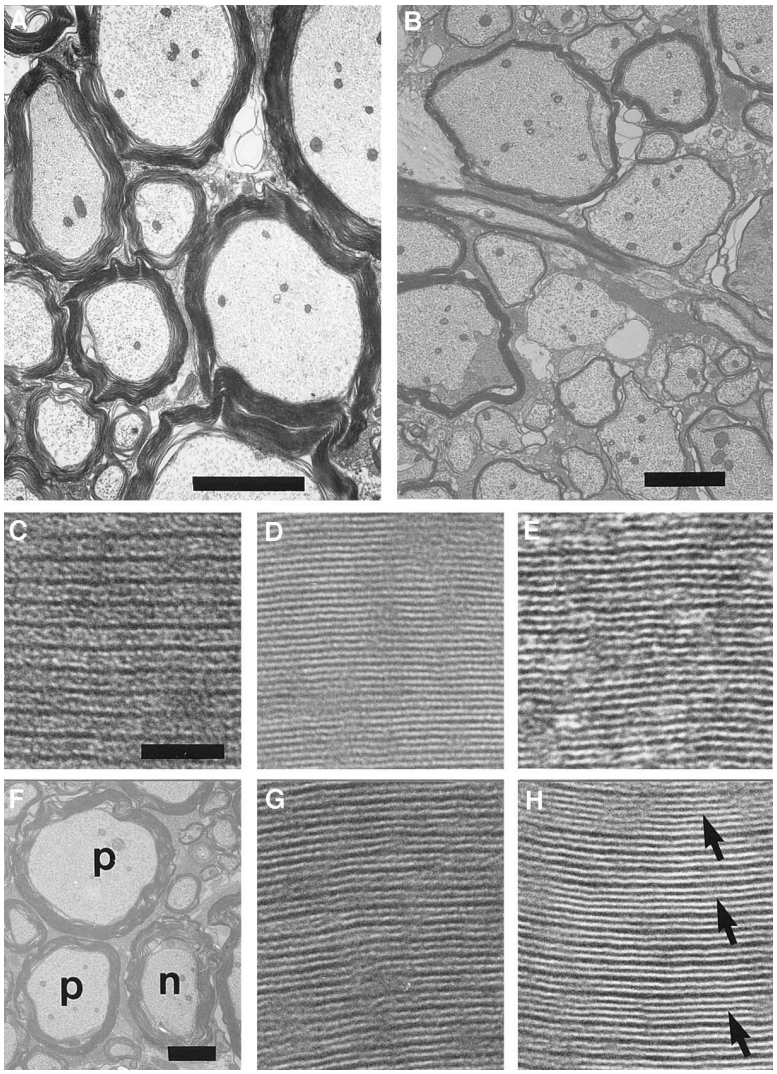

Figure 4. Ultrastructure of CNS Myelin in PLP Mutant Alleles

(A) Electron micrograph of spinal cord from adult plp^{null}/Y mice shows axons surrounded by compacted myelin sheaths of appropriate thickness. Axons of large and small diameter are myelinated. Scale bar = 2 μm.

(B) In comparison with the well-myelinated tissue shown in (A), the spinal cord of an adult *rumpshaker* mouse (plp^{rsh}/Y) is severely dysmyelinated. Many axons are naked or thinly myelinated. Note that plp^{rsh} represents the least severe phenotype of the spontaneous plp mutant mice. Scale bar = 2 μm.

(C–E) Myelin sheaths from wild-type (C), plp−/Y (D), and plp^{ip} mice (E) show differences in periodicity of myelin. Note that the IPL is condensed in plp^{null} mice, resembling the MDL. Scale bar = 50 nm.

(F–H) Spinal cord from a chimeric female (plp+/−). A section immediately adjacent to the ultrathin section was immunostained for PLP (not shown), allowing the identification of two PLP-positive (p) fibers and one PLP-negative fiber (n). Myelin sheaths of a PLP-positive (G) and a PLP-negative (H) fiber are shown. The arrows (H) indicate regions where the distiction between the IPL and MDL is lost. Same scale as in (C).

PMP22) were not induced in oligodendrocytes (data not shown). We also immunostained blots for the two DM20 homologs, M6A and M6B. Both proteins were detected by Western blot analysis of purified myelin, however, at a low abundance. M6A (but not M6B) was about 2-fold more abundant in mutant mice relative to controls. This was unexpected because M6A expression previously has not been associated with oligodendrocytes (Lagenaur et al., 1992). Our results were confirmed with independent myelin preparations, but the low overall abundance of M6A relative to PLP/DM20 suggests that this increase is not a sufficient compensatory mechanism. It also cannot be formally excluded that M6A immunoreactivity derives from contaminating axonal membranes. All of these observations in the adult brain cannot rule out the existence of compensatory mechanisms at earlier stages of oligodendrocyte development.

Other Changes

In general, the CNS and PNS of plp−/Y mice were indistinguishable from wild type at all ages studied (up to 1 year). Although the majority of axons were normal, we noted some axonal spheroids, particularly in mice older than about 2 months, predominantly in small diameter axons, throughout the CNS (not shown). The significance of axonal swellings, which have been reported in several of the natural PLP mutants, is uncertain and under investigation at present.

MBP*PLP Double-Mutant Mice

Neither a mutation of the PLP gene nor of the MBP gene blocks the assembly of CNS myelin completely. Can the spiral wrapping of membranes proceed in the absence of both proteins? We have crossed the plp^{null} allele with *shiverer* (shi) mice to generate double-mutant mice lacking both proteins. Although shi/shi and shi/shi*plp−/Y mice exhibited a very similar phenotype with ataxia and tremors, it was striking that all double mutants were long-lived (>6 months), whereas shi/shi mice died prematurely at about 3 months of age. The morphological basis for this finding awaits to be identified, as the overall appearance of double-mutant mice (Figure 6A) was very similar or identical to that of the natural shi/shi phenotype. Many axons were naked, and any sheaths present were thin. Also in common with *shiverer*, the myelin of double mutants was frequently decompacted, lacking an MDL.

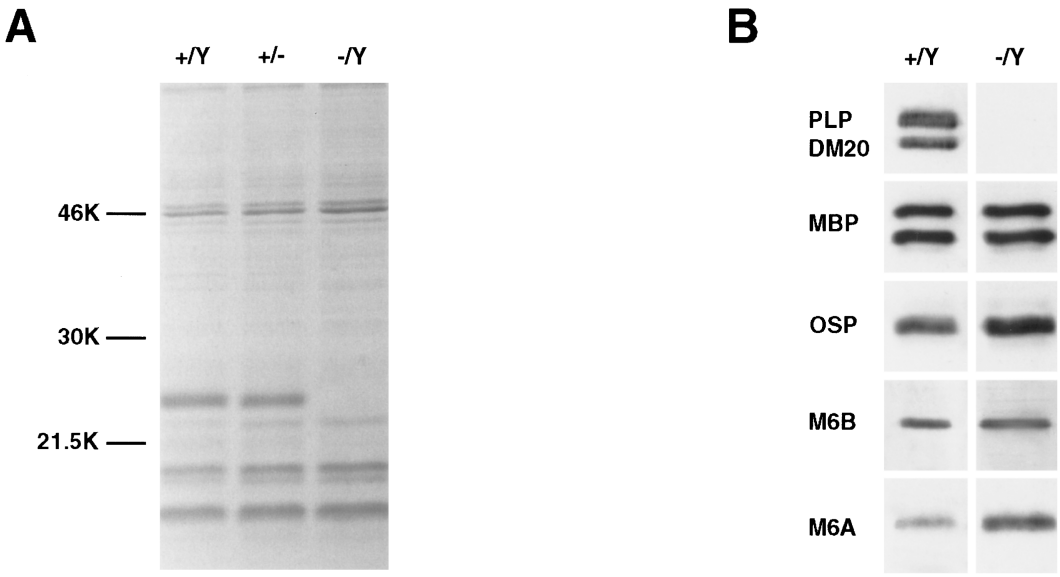

Figure 5. Myelin Proteins in plp^{null} Mice

(A) Coomassie Blue staining of total protein (5 μg/lane) from purified myelin demonstrates the absence of PLP and DM20 in plp^{null} (−/Y) mutants in comparison to wild-type controls (+/Y). There is no compensatory upregulation of other myelin proteins. PLP has a relative mobility of 24 kDa as shown (Lees and Brostoff, 1984), and DM20 (relative mobility: 20 kDa) is not stained as efficiently. MBP isoforms are prominent. (B) Western blot analysis of known membrane proteins (indicated on the left) in purified myelin of adult plp^{null} mutants (−/Y) and wild-type controls (+/Y) (10 μg/lane). Peripheral myelin proteins are absent (not shown). Note that the neuronal M6A protein is detected at about a 2-fold higher level but at a very low overall abundance.

However, the IPL was identifiable and often of increased density, similar to that of the plp−/Y mice (Figure 6B).

Discussion

The normal function of PLP/DM20 has remained obscure because mutations of its gene are associated with an unusually wide spectrum of pathological abnormalities (Nave and Boespflug-Tanguy, 1996). It has been speculated that the pleiotropic defects reported for *jimpy* or *rumpshaker* mice and other rodent mutants (modeling Pelizaeus-Merzbacher disease and SPG-2 in humans) result from the complicated interaction of a loss-of-function and a gain-of-function effect, but the relative contribution of each is unknown. We have experimentally uncoupled the two disease processes by completely eliminating expression of a targeted PLP gene in mice and have compared this new mutation with previously identified alleles. Clearly, mice that have no coding capacity for PLP or PLP-related polypeptides differ at the molecular, cellular, and behavioral level.

The Function of PLP/DM20 in Myelin

Most important, with respect to PLP function, is the observation that all mutant oligodendrocytes differentiate completely and spirally enwrap myelination-competent axons, irrespective of their size. At the electron microscopic level, intra- and extracellular membrane appositions are clearly visible. Over a period of 1 year, compacted myelin displays no direct or indirect signs of premature breakdown in vivo. Moreover, in MBP*PLP-deficient double-mutant mice, the IPL but not the MDL is preserved. If any loosening of the IPL were genuine in these mice, a complete disintegration of myelin membranes would be expected.

However, the specific ultrastructural defects of myelin in PLP-deficient mice processed for electron microscopy are informative and suggest a function of proteolipids in the myelin architecture. The extracellular compaction of adjacent membranes appears abnormally condensed (so that in most regions of a sheath, the MDL and IPL are difficult to distinguish). This feature resembles other "PLP-deficient" mutants (Duncan et al., 1987; 1989; Schneider et al., 1995), is in line with X-ray diffraction data (Kirschner et al., 1984), and can be correlated with a markedly reduced stability of the myelin sheath. PLP-deficient myelin, although compacted in vivo, is extrasensitive to the osmotic stress during perfusion–fixation, yielding more "fixation artifacts" than normal myelin. Such a difference in physical stability has been convincingly documented in the CNS of chimeric females in which PLP-positive and -negative myelin sheaths could be processed under identical conditions.

Our findings challenge the previously held view that PLP is required to assemble compacted myelin, a model that was self-suggestive given the abundance of this protein. For comparison, such a critical function was expected for MBP and for P0 (in peripheral myelin) and has been confirmed with the corresponding mutants (Readhead et al., 1987; Giese et al., 1992). We propose that PLP/DM20 is not primarily responsible for membrane compaction, serving a different cellular function than P0. Likewise, there is no in vitro evidence that PLP has the same adhesive properties as P0 (Filbin et al., 1990). However, proteolipids may well engage in homophilic interactions, forming "struts" that expand the width of the IPL and bridge the extracelluar gap (see

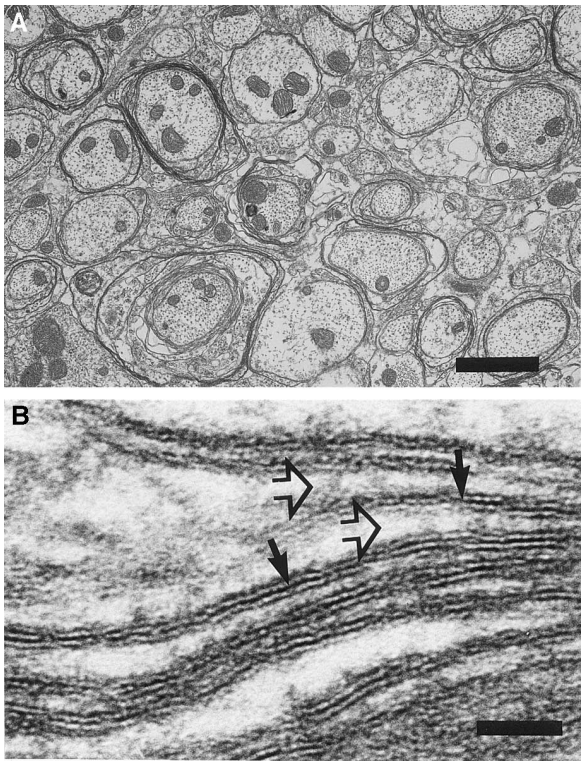

Figure 6. Myelin Ultrastructure of PLP*MBP Double-Mutant Mice

Spinal cord from an mbp−/−*plp−/y mouse shows marked dysmyelination, similar to that seen in *shiverer* mice. Axons have either no myelin sheaths or thin, poorly compacted sheaths. Ultrastructure of the sheath shows splitting and nonfusion at the MDL (open arrows), typical of the homozygous *shiverer*. Note that the IPL is formed in the absence of PLP/DM20 as a single fused line and appears as a denser structure (closed arrows). Scale bars: A = 2 μm, and B = 50 nm.

also Kitagawa et al., 1993; Yoshida and Colman, 1996). Such specialized interactions may require the prior association of the two membranes to engage. We propose that the primary junctions are stabilized by secondary PLP/DM20-dependent bonds, a mechanism perhaps modeled best as a "PLP-zipper", which must be firmly aligned before it can be closed.

Comparison of PLP Mutant Mice

Previously characterized PLP mutations have a wide range of phenotypic expression (Nave and Boespflug-Tanguy, 1996). It is important to compare the results presented here with a previous report of PLP gene targeting (Boison and Stoffel, 1994). In that study, two mutants (*plp*^{neo} and *dm20*^{neo}) were designed as "isoform-specific" knockouts; however, their molecular analysis revealed an unpredicted and novel defect of RNA splicing: intron 3, containing an inserted neo gene, is not spliced out (Figure 1 of Boison et al., 1995). Because the ninth in-frame codon of intron 3 introduces a *stop* into the open reading frame (Ikenaka et al., 1988), the abnormal splice products of *plp*^{neo} and *dm20*^{neo} mice encode PLP-related proteins of 159 and 124 residues, respectively. Comparable defects of PLP mRNA splicing are known in mouse and man, but the phenotype of *plp*^{neo} and *dm20*^{neo} mice is much less severe (Boison and Stoffel, 1994). It has been pointed out that "antisense" transcription of the neo gene, starting about 10 kb downstream of the PLP transcription start site, lowers the steady state level of PLP mRNA (Figure 3 of Boison et al., 1995). Genetically, *plp*^{neo} mice are therefore more complex than the natural PLP mutants because abnormal RNA splicing and reduced gene expression overlap. Truncated polypeptides were not detected in purified myelin (Boison and Stoffel, 1994) presumably because they are abnormally folded, retained in the endoplasmic reticulum (ER), and rapidly degraded (Roussel et al., 1987; Hammond and Helenius, 1994; Gow et al., 1994). A comparable RNA splice defect has been carefully studied in the *jimpy* mouse, in which truncated proteolipids are extremely difficult to detect (Yanagisawa and Quarles, 1986; Benjamins et al., 1994; Fannon et al., 1994). *Plp*^{neo} and *dm20*^{neo} mice synthesize myelin membranes but fail to compact them. This allows MAG immunoreactivity to spread widely (Figure 4 of Boison et al., 1995), compared to the periaxonal localization of MAG in the wild-type (Martini and Schachner, 1986) and in the null allele (this study). Interestingly, a reinvestigation of the mutant strain suggested that myelin disruption was partly artifactual (Rosenbluth et al., 1996). Regardless of the true myelin morphology, oligodendrocytes in plp^{neo} mice failed to myelinate the majority of small-caliber axons in the optic nerve (Figure 7 of Boison et al., 1995) and spinal cord. Dysmyelination caused significant motor defects, as documented with the rotarod test (Figure 6 of Boison et al., 1995), and nerve conduction velocities were reduced (Gutierrez et al., 1995).

PLP-Related Polypeptides and CNS Dysmyelination

A comparison of all of the mutations suggests that even low amounts of truncated (but PLP-related) polypeptides act as effective inhibitors of myelination. This is supported by complementation experiments in which the *jimpy* mutation had emerged as genetically dominant over an autosomal wild-type PLP transgene (Nadon et al., 1994; Schneider et al., 1995). Comparing the phenotype of various mutant alleles (as summarized in Table 1) with the ability of each to encode a gene product, we conclude that dysmyelination, as a disorder of myelin synthesis, strictly depends on the expression of PLP or PLP-related polypeptides, and that it constitutes a "continuum" of disease expression. In the order of increasing severity, the pathological changes are (1) the inability of oligodendrocytes to recognize and myelinate small-caliber axons, (2) the premature arrest of myelination, with abnormally thin sheaths, (3) the failure to recognize and myelinate large-caliber axons, and (4) oligodendrocyte death with features of apoptosis. These findings correlate with an increasing "clinical" severity from locomotor defects to tremors, seizures, and premature death.

PLP Toxicity

In *jimpy* mice, >90% of oligodendrocytes are eliminated by cell death, coinciding with expression of abnormally

Table 1. Mutations in the PLP Gene and Phenotypes Differ Widely in the Mouse and Have Been Grouped by Increasing Clinical Severity and the Absence or Presence of Protein Coding Capacity

Genotype	Polypeptide encoded	Abnormal motor development	Dysmyelination[7] of CNS axons	Abnormal oligodendrocyte death	Myelin structure[8]	Reference
plp^{null}	none[4]	Not detectable	Absent	No	Compacted, condensed IPL, reduced stability	This study
plp^{neo}	159aa[1,4]	Mild	Small caliber	No	Uncompacted[9]	Boison and Stoffel, 1995
plp^{rsh}	276aa[2,5]	Moderate	Small and large caliber		Compacted	Schneider et al., 1992
plp^{jp}	242aa[1,4]	Severe (lethal)	Most axons	Increased	Compacted	Duncan et al., 1989
plp^{msd}	276aa[3,4]				Condensed IPL	Skoff, 1995
plp-transgenic	276aa[6]				Compacted	Readhead et al., 1994

The number of predicted amino acids (aa) is indicated and can deviate from full-length PLP (276aa) as a result of abnormal RNA splicing.[1] Single amino acid substitutions[2,3] are Ile^{186}→Thr and Ala^{242}→Val, respectively. PLP is coexpressed with DM20 (241aa, not indicated), except in the isoform-specific plp^{neo} and $dm20^{neo}$ alleles. Steady-state RNA levels are either strongly reduced[4] (<10% of wild type) or in the normal range[5] (60%). PLP–transgenic mice overexpress[6] normal PLP/DM20 mRNA (>150%). Dysmyelination[7] is defined as a missing or abnormally thin axonal ensheathement. Myelin structure[8] refers to the ultrastructural features of myelinated axons (IPL, intraperiod line). For plp^{neo} mice[9], different results were reported by Boison et al. (1995) and Rosenbluth et al. (1996). For additional references, see Nave (1995).

spliced PLP mRNA (Skoff, 1995). Combined with our results and those of Boison et al. (1995), this could be explained by assuming that *jimpy*–PLP forms toxic "junk" that perturbs cellular trafficking. However, cloned *jimpy*–PLP cDNA has been overexpressed in transiently transfected COS7 cells, and the encoded polypeptide, which is retained in the ER, could be immunostained in live cells days after transfection (Jung et al., 1996, and data not shown). This indicates that the toxicity of misfolded PLP is cell-type specific. Could there be another link between PLP and oligodendrocyte death? It is tempting to speculate that prior to myelination, wild-type PLP (or DM20) associates with other intracellular proteins that are involved in oligodendrocyte differentiation. When retained in the ER, misfolded (but PLP-related) polypeptides may associate with the same proteins altering their function, possibly by being jointly degraded. The model predicts that the misfolded polypeptides in dysmyelinated mutants must have a minimum length to maintain a structural homology with wild-type PLP/DM20. It could explain why an abnormal splice product of *jimpy* mice (encoding 242 residues with three transmembrane domains) is more "toxic" than the splice product of plp^{neo} mice (159 residues, two transmembrane domains). In all of the other rodent mutants, the size of PLP (276 residues) is unaltered.

Mouse Models of Human Diseases

The primary structure of PLP and DM20 is 100% conserved between mouse and man. PMD (McKusick 312080) has been associated with numerous mutations of the human PLP gene, and some mutations cause spastic paraplegia (SPG-2, McKusick 312920), a less severe and clinically distinct entity. At least one mutation (Ile^{186}→Thr) is identical in mouse (plp^{rsh}) and man (SPG-2) (Schneider et al., 1992; Kobayashi et al., 1994). These genetic homologies provide an opportunity to investigate whether expression of the disease phenotype is also the same.

Our present data suggest that the same mutation can have different consequences for mouse and man. Raskind et al. (1991) have analyzed a patient diagnosed with PMD and revealed a deletion of his PLP gene, comprising a human null allele. Retarded motor development, as first signs of a disease, were noticed at about 1 year of age, and hypomyelination was diagnosed by magnetic resonance imaging several years later. The patient is now in his 40s and is wheelchair-bound (T. Bird, personal communication). A nonsense mutation found in another patient diagnosed with SPG-2 interrupts the PLP reading frame after a few nucleotides and must be equivalent to a null allele (O. Boespflug-Tanguy, personal communication). Thus, complete loss of the PLP gene function is not tolerated in humans, causing a mild form of PMD/SPG-2 with late onset and slow progression. Are there fundamental differences between mouse and human myelin? The biochemical composition is nearly identical (Lees and Brostoff, 1984), and it is unlikely that PLP, highly conserved in evolution, serves different functions in different mammalian species. The incorporation of PLP increases the physical stability of compacted myelin, but PLP-deficient myelin in mice is stable in vivo for at least 1 year, as shown here, and possibly longer. We suggest that PLP is more relevant for humans because they are long-lived. In humans, myelin assembly begins around birth and continues for several years. We hypothesize that in the absence of proteolipids, myelin is at a high risk of premature breakdown and will degenerate within a few years and with a similar (absolute) time course lasting several years. Such a disease is expected to show features of a developmental disorder in children (PMD/SPG-2), because it interferes with their normal cognitive and motor development. In contrast, the plp^{null} allele of the mouse has no functional consequences within its reproductive age but may become manifest as a late-onset neurodegenerative disease in animals >1 year old. For comparison, the known developmental defects of myelination (such as the connatal form of PMD or dysmyelination in *jimpy* mice) have a species-specific time course: the human disease process is "squeezed" into the first postnatal weeks of the mouse. We are further investigating preliminary observations that degenerative myelin changes surface in the plp^{null} allele of

aged mice. It is anticipated that this issue of disease progression versus time will be relevant for other mouse models of human genetic disorders and the understanding of pathogenic mechanisms.

Experimental Procedures

Molecular Cloning

Overlapping clones of the PLP gene were obtained by screening a mouse Sv129 genomic library (Stratagene) with probes corresponding to the 5′ flanking region and the 3′UTR obtained from a mouse PLP cDNA (Nave et al., 1987). A targeting vector for positive–negative selection (Mansour et al., 1988) was constructed by first subcloning a KpnI-BamHI fragment ('long arm') comprising most of introns 1–3 into vector pSP72 (Promega). Next, the neomycin resistance gene (from pMCneopA, Stratagene) was cloned 5′ to the long arm in antisense orientation. For negative selection, the HSV-TK gene (from pMC1TK, Stratagene) was inserted XhoI-BamHI at the 3′ end of the construct. Finally, a 1.5 kb BamHI fragment ('short arm') comprising the PLP promoter and upstream part of the 5′UTR was inserted. In the resulting targeting construct, critical parts of the 5′UTR between the BamHI site of exon 1 and the most 5′ KpnI site of intron 1 were deleted, including the translation start site.

Selection of ES Cells

R1 mouse ES cells were kindly provided by A. Nagy (Toronto) and cultured on mitomycin-treated primary mouse embryonic fibroblasts. For electroporation (BioRad Gene Pulser; 240 V; 500 or 960 mF), 10^7 ES cells were suspended in 0.8 ml phosphate-buffered saline (PBS), containing 50 μg of the linearized (XhoI) targeting construct. Transfected cells were cultured on gelatinized dishes (Falcon), and double selection with 300 μg/ml G418 (Gibco) and 2 mM gancyclovir was performed after 48 and 72 hr, respectively; 8–10 days after electroporation, double-resistant colonies were picked and trypsinized. About one third of each colony was plated onto feeder cells. The remaining two thirds of eight clones each were pooled and washed in PBS, suspended in 50 μl water, heat-lysed at 95°C (for 10 min), and digested with 10 μg proteinase K (for 30 min at 55°C).

To identify homologous recombinants, aliquots of the pooled lysates were used to PCR amplify a 1.7 kb genomic fragment in a 50 μl reaction. The forward primer (sB4ext) corresponded to a PLP genomic sequence localized immediately upstream of the 5′ homology region (5′-AGTCTGTGTCTGGAGAGCAG-3′). A reverse primer (MKneo1) was derived from the *neo* gene (5′-TACGGTATCGCCGCT CCCGATTCGCA-3′). Denaturation was at 94°C (for 60 s), annealing at 56°C (for 45 s), and extension at 72°C (for 60 s). Amplification products were verified by Southern analysis, using a 1.5 kb BamHI fragment as a ^{32}P-labeled 5′-probe. Individual PCR-positive clones were confirmed by Southern analysis. Size-separated DNA (10 μg) was blotted and hybridized either to the 5′ probe or to a 1.1 kb XhoI/BamHI fragment of pMCneo. Microinjection of selected ES cells into C57BL/6J blastocysts was performed by standard procedures. Highly chimeric males were crossed to C57BL/6J females. Heterozygous mutants were crossed with C57BL/6J males to obtain hemizygous mutants.

For routine analysis, offspring were genotyped by PCR. Absence of the wild-type allele was shown with sB4ext as a forward primer and PLP5′a as the reverse primer (5′-CTGTTTTGCGGCTGACT TTG-3′), the latter corresponding to the upstream part of exon 1 that is absent from the mutant allele. The targeted allele was positively identified with primers neo4 (5′-GGCTATTCGGCTATGACTG GGC-3′) and neo5 (5′-GGGTAGCCAACGCTATGTCCTG-3′), yielding a 620 bp product specific for the inserted neo gene.

Transgenic Complementation

Transgenic complementation of the plp^{null} allele was achieved by breeding heterozygous carriers with male mice (lines #66 and 72), transmitting an autosomal wild-type PLP transgene (Readhead et al., 1994). Presence of the transgene was revealed by amplification of a 250 bp genomic fragment obtained with the forward primer COS3′ (5′-CAGGTGTTGAGTCTGATCTACACAAG-3′) at the 3′ end of the transgene and reverse primer T7cos (5′-GCATAATACGACTC ACTATAGGGATC-3′) at its 3′ end, as previously described.

MBP*PLP Double Mutants

Double mutant shi/shi*plp−/Y mice were obtained by breeding homozygous *shiverer* males (kindly provided by J. Trotter) with homozygous plp−/− females and brother–sister mating of double-heterozygous animals. Presence of the wild-type and mutant MBP alleles was detected with two sets of specific primers (Gomez et al., 1990). One primer pair was derived from intronic sequences flanking exon 6 of the normal MBP gene (forward: 5′-AGCTCTGGTCTTTCTTG CAG-3′, reverse: 5′-CCCCGTGTAGGAATATTACATAAC-3′), producing a 169 bp fragment. The *shiverer* allele was identified as a 380 bp fragment with primers complementary to sequences on either side of the break point located in intron 2 (forward: 5′-CAGGGGATG GGGAGTCAGAAGTGAG-3′, reverse: 5′-ATGTATGTGTGTGTGTGC TTATCTAGTGTA-3′).

Motor Performance Assay

The 'rotarod-test' utilized a motor-driven metal roller (2 cm diameter × 10 cm wide) flanked by two larger plates. Male hemizygous mutant mice (n = 6) and the same number of age-matched controls were analyzed at 6 months of age and again at 12 months. As additional controls, we used 6-month-old *rumpshaker* mice (n = 6) partly rescued with one copy of the autosomal PLP gene of line #66 (Readhead et al., 1994; A. Schneider et al., unpublished data). All mice were placed on the roller at rest. After 15 s, the rotarod was started at 1 round per min (rpm). In 60 s intervals, the rotating speed was successively inceased to 2, 4, 8, 12, 16, and 20 rpm. In a series of five trials per animal, the time (in seconds) that the mice remained on the roller was scored.

RNA Analysis

Total RNA was isolated from brains of 4-month- and 6-month-old mice (RNeasy, Quiagen). For Northern analysis, RNA was size fractionated on a 1% denaturing agarose gel (10 μg/lane) before blotting onto nylon membranes (Nytran). Radiolabeled probes were generated by random prime labeling of a mouse PLP cDNA (Nave et al., 1987). Hybridization was performed at 42°C in the presence of 50% formamide, 5× Denhardts, 3×SSC, 120 mM phosphate, 1% SDS, 200 ng/ml salmon sperm DNA, and 10^6 cpm/ml radiolabeled probe. Blots were washed to a stringency of 0.2×SSC at 55°C and autoradiographically exposed to Kodak X-AR5 film with intensifying screens (24–48 hr).

Protein Analysis

Total brain extracts were made from 200 mg fresh tissue in 7 ml PBS, 1% SDS, using a polytron homogenizer at the highest setting (10 s). The homogenate was immediately boiled for 3 min, and insoluble material was pelleted by centrifugation. Myelin was isolated from homogenized brains in 0.32 M sucrose (Norton, 1974). Equal amounts of protein (10 μg) were size separated on denaturing 12% SDS–polyacrylamide gels and transferred to supported nitrocellulose membranes (BA-S 85, Schleicher and Schüll) by semidry electroblotting. Membranes were blocked with 5% nonfat dry milk (in PBS, 0.1% Tween-20) for 1 hr at room temperature. Incubation with antibodies (in PBS containing 2% nonfat dry milk) was for 1 hr, followed by a wash and 1 hr incubation with a horseradish peroxidase-conjugated secondary antibody (Amersham), diluted 1:1000 in the same buffer. Immunoreactive protein was detected with an enhanced chemiluminescence kit (ECL, Amersham) according to the manufacturer's instructions, using ECL-Hyperfilm (Amersham). Western blots were stripped and reprobed with different antibodies. The M6A antipeptide antibody M6–7 has been described (Lagenaur et al., 1992) and was diluted 1:10. Antibodies against MBP (Boehringer) were diluted 1:500; anti-GFAP, 1:250 (Serva); anti-PO, 1:1000; anti-OSP, 1:100; anti-M6B, 1:10 (kindly provided by H. Werner); and PLP/DM20, 1:50, respectively. The PLP antibody (A431) is directed against the PLP C-terminus (Jung et al., 1996). For total protein analysis, 5 μg of protein was separated on a 12% SDS–polyacrylamide gel and visualized by silver staining and with Coomassie Brilliant Blue.

Histology

Mice were perfused through the left ventricle with saline followed by a modified Karnovsky fixative with 5% glutaraldehyde–4% paraformaldehyde in cacodylate buffer (pH 7.2) (Griffiths et al., 1981). Tissues were removed and maintained in the same fixative before routine processing for embedding in Araldite. Sections (1 μm) were stained with methylene blue–azure II, or grids (60 nm) were stained with uranyl acetate and lead citrate. Other mice were perfused with buffered neutral formalin, and tissues were embedded in paraffin. Immunostaining was performed on 1 μm resin sections or 8 μm paraffin sections using the PAP technique. In situ hybridizations on 6 μm paraffin sections were performed by standard procedures using ^{35}S-labeled riboprobes spanning the PLP coding region and 5′ untranslated region (Milner et al., 1985).

Acknowledgments

Correspondence should be addressed to K. A. N. (e-mail: nave@sun0.urz.uni-heidelberg.de). We thank H. Krischke, J. M. Barrie, and M.C. McCulloch for excellent technical assistance. Various antibodies were kindly provided by J. Archelos (P0), J. Bronstein (OSP), N. Groome (PLP), C. Lagenaur (M6A), J.-M. Matthieu (MBP), R. Quarles (MAG), and M. Schwab (rMAL). We also thank A. Nagy for providing R1-ES cells, J. Trotter for *shiverer* mice, and M. Jung, M. Rossner, and H. Werner for critical reading of the manuscript. This work was supported by grants from the Deutsche Forschungsgemeinschaft (SFB317) and the EC Biomed-2 program to K. A. N. and Action Research to I. G.

Received November 18, 1996; revised December 19, 1996.

References

Baumrind, N.L., Parkinson, D., Wayne, D.B., Heuser, J.E., and Pearlman, A.L. (1992). EMA: a developmentally regulated cell-surface glycoprotein of CNS neurons that is concentrated at the leading edge of growth cones. Dev. Dyn. *194*, 311–325.

Benjamins, J.A., Studzinski, D.M., and Skoff, R.P. (1994). Analysis of myelin proteolipid protein and F0 ATPase subunit 9 in normal and jimpy CNS. Neurochem. Res. *19*, 1013–1022.

Boison, D., and Stoffel, W. (1994). Disruption of the compacted myelin sheath of axons of the central nervous system in proteolipid protein-deficient mice. Proc. Natl. Acad. Sci. USA *91*, 11709–11713.

Boison, D., Büssow, H., D'Urso, D., Müller, H.W., and Stoffel, W. (1995). Adhesive properties of proteolipid protein are responsible for the compaction of CNS myelin sheaths. J. Neurosci. *15*, 5502–5513.

Braun, P. (1984). Molecular organization of myelin. In *Myelin*, 2nd edition, P. Morell, ed. (New York: Plenum Press), pp. 97–116.

Bunge, R.P., and Fernandez-Valle, C. (1995). Basic biology of the Schwann cell. In *Neuroglia*, H. Kettenmann, and B. R. Ransom, eds. (New York: Oxford University Press), pp. 44–57.

Campagnoni, A. (1995). Molecular biology of myelination. In *Neuroglia*, H. Kettenmann, and B. R. Ransom, eds. (New York: Oxford University Press), pp. 555–570.

Carango, P., Funanage, V.L., Quiros, R.E., Debruyn, C.S., and Marks, H.G. (1995). Overexpression of DM20 messenger RNA in two brothers with Pelizaeus-Merzbacher disease. Ann. Neurol. *38*, 610–617.

Dickinson, P.J., Fanarraga, M.L., Griffiths, I.R., Barrie, J.A., Kyriakides, E., and Montague, P. (1996). Oligodendrocyte progenitors in the embryonic spinal cord express DM-20. Neuropathol. Appl. Neurobiol. *22*,188–198.

Duncan, I.D., Hammang, J.P., and Trapp, B.D. (1987). Abnormal compact myelin in the myelin-deficient rat: absence of proteolipid protein correlates with a defect in the intraperiod line. Proc. Natl. Acad. Sci. USA *84*, 6287–6291.

Duncan, I.D., Hammang, J.P., Goda, S., and Quarles, R.H. (1989). Myelination in the jimpy mouse in the absence of proteolipid protein. GLIA *2*, 148–154.

Ellis, D., and Malcolm, S. (1994). Proteolipid protein gene dosage effect in Pelizaeus-Merzbacher disease. Nat. Genet. *6*, 333–334.

Fannon, A.M., Mastronardi, F.G., and Moscarello M.A. (1994). Isolation and identification of proteolipid proteins in *jimpy* mouse brains. Neurochem. Res. *19*, 1005–1012.

Filbin, M.T., Walsh, F.S., Trapp, B.D., Pizzey, J.A., and Tennekoon, G.I. (1990). Role of myelin P0 protein as a homophilic adhesion molecule. Nature *344*, 871–872.

Giese, K.P., Martini, R., Lemke, G., Soriano, P., and Schachner, M. (1992). Disruption of the P0 gene in mice leads to abnormal expression of recognition molecules, and degeneration of myelin and axons. Cell *71*, 565–576.

Gomez, C.N., Muggleton-Harris, A.L., Whittingham, D.G., Hood, L.E., and Readhead, C. (1990). Rapid preimplantation detection of mutant (shiverer) and normal alleles of the mouse myelin basic protein gene allowing selective implantation and birth of live young. Proc. Natl. Acad. Sci. USA *87*, 4481–4484.

Gow, A., Friedrich, V.L., and Lazzarini, R.A. (1994). Many naturally occurring mutations of myelin proteolipid protein impair its intracellular transport. J. Neurosci. Res. *37*, 574–583.

Griffiths, I.R., Duncan, I.D., and McCulloch, M. (1981). Shaking pup: a disorder of central myelination in the spaniel dog. II. Ultrastructural observations on the white matter of cervical spinal cord. J. Neurocytol. *10*, 847–858.

Gutierrez, R., Boison, D., Heinemann, U., and Stoffel, W. (1995). Decompaction of CNS myelin leads to a reduction of the conduction velocity of action potentials in optic nerves. Neurosci. Lett. *195*, 93–96.

Hammond, C., and Helenius, A. (1994). Quality control in the secretory pathway: retention of a misfolded viral membrane glycoprotein involves cycling between the ER, intermediate compartment, and Golgi apparatus. J. Cell Biol. *126*, 41–52.

Hodes, M.E., Pratt, V.M., and Dlouhy, S.R. (1994). Genetics of Pelizaeus-Merzbacher disease. Dev. Neurosci. *15*,383–394.

Hudson, L.D., Berndt, J.A., Puckett, C., Kozak, C.A., and Lazzarini, R.A. (1987). Aberrant splicing of proteolipid protein mRNA in the dysmyelinating jimpy mutant mouse. Proc. Natl. Acad. Sci. USA *84*, 1454–1458.

Ikenaka, K., Furuichi, T., Iwasaki, Y., Moriguchi, A., Okano, H., and Mikoshiba, K. (1988). Myelin proteolipid protein gene structure and its regulation of expression in normal and *jimpy* mutant mice. J. Mol. Biol. *199*, 587–596.

Ikenaka, K., Kagawa, T., and Mikoshiba, K. (1992). Selective expression of DM-20, an alternatively spliced myelin proteolipid protein gene product, in developing nervous system and in nonglial cells. J. Neurochem. *58*, 2248–2253.

Inoue, K., Osaka, H., Sugiyama, N., Kawanishi, C., Onishi, H., Nezu, A., Kimura, K., Kimura, S., Yamada, Y., and Kosaka, K. (1996). A duplicated PLP gene causing Pelizaeus-Merzbacher disease detected by comparative multiplex PCR. Am. J. Hum. Genet. *59*, 32–39.

Jung, M., Sommer, I., Schachner, M., and Nave, K.-A. (1996). Monoclonal antibody O10 defines a conformationally sensitive cell-surface epitope of proteolipid protein (PLP): evidence that PLP misfolding underlies dysmyelination in mutant mice. J. Neurosci. *16*, 7920–7929.

Kagawa, T., Ikenaka, K., Inoue, Y., Kuriyama, S., Tsujii, T., Nakao, J., Nakajima, K., Aruga, J., Okano, H., and Mikoshiba, K. (1994). Glial cell degeneration and hypomyelination caused by overexpression of myelin proteolipid protein gene. Neuron *13*, 427–442.

Kirschner, D., Ganser, A.L., and Caspar, D.L.D. (1984). Diffraction studies of molecular organization and membrane interactions in myelin. In *Myelin*, 2nd edition, P. Morell, ed. (New York: Plenum Press), pp. 51–95.

Kitagawa, K., Sinoway, M.P., Yang, C., Gould, R.M., and Colman, D.R. (1993). A proteolipid protein gene family: expression in sharks and rays and possible evolution from an ancestral gene encoding a pore-forming polypetide. Neuron *11*, 433–448.

Knapp, P.E., Skoff, R.P., and Redstone, D.W. (1986). Oligodendroglial cell death in jimpy mice: an explanation for the myelin deficit. J. Neurosci. *6*, 2813–2822.

Kobayashi, H., Hoffman, E.P., and Marks, H.G. (1994). The *rumpshaker* mutation in spastic paraplegia. Nat. Genet. *7*, 351–352.

Lagenaur, C., Kuenemund, V., Fischer, G., Fushiki, S., and Schachner, M. (1992). Monoclonal M6 antibody interferes with neurite extension of cultured neurons. J. Neurobiol. *23*, 71–88.

Lees, M., and Brostoff, S.L. (1984). Proteins of myelin. In *Myelin*, 2nd edition, P. Morell, ed. (New York: Plenum Press), pp. 197–224.

Lupski, J.R., Chance, P.F., and Garcia, C.A. (1993). Inherited primary peripheral neuropathies. JAMA *270*, 2326–2330.

Mansour, S.L., Thomas, K.R., and Capecchi, M.R. (1988). Disruption of the proto-oncogene int-2 in mouse embryo–derived stem cells: a general strategy for targeting mutations to non-selectable genes. Nature *336*, 348–352.

Martini, R., and Schachner, M. (1986). Immunoelectron microscopic localization of neural cell adhesion molecules (L1, N-CAM, and MAG) and their shared carbohydrate epitope and myelin basic protein in developing sciatic nerve. J. Cell Biol. *103*, 2439–2448.

Martini, R., Mohajeri, M.H., Kasper, S., Giese, K.P., and Schachner, M. (1995). Mice doubly deficient in the genes for P0 and myelin basic protein show that both proteins contribute to the formation of the major dense line in peripheral nerve myelin. J. Neurosci. *15*, 4488–4495.

Milner, R.J., Lai, C., Nave, K.-A., Lenoir, D., Ogata, J., and Sutcliffe, J.G. (1985). Nucleotide sequences of two mRNAs for rat brain myelin proteolipid protein. Cell *42*, 931–939.

Nadon, N., Arnheiter, H., and Hudson, L.D. (1994). A combination of PLP and DM20 transgenes promotes partial myelination in the jimpy mouse. J. Neurochem. *63*, 822–833.

Nave, K.-A. (1995). Neurological mouse mutants: a molecular genetic analysis of myelin proteins. In *Neuroglia*, H. Kettenmann, and B. Ransom, eds. (New York: Oxford University Press), pp. 571–586.

Nave, K.-A., and Boespflug-Tanguy, O. (1996). Developmental defects of myelin formation: from X-linked mutations to human dysmyelinating diseases. Neuroscientist *2*, 33–43.

Nave, K.-A., Lai, C., Bloom, F.E., and Milner, R.J. (1986). Jimpy mutant mouse: a 74-base deletion in the mRNA for myelin proteolipid protein and evidence for a primary defect in RNA splicing. Proc. Natl. Acad. Sci. USA *83*, 9264–9268.

Nave, K.-A., Lai, C., Bloom, F.E., and Milner, R.J. (1987). Splice site selection in the proteolipid protein (PLP) gene transcript and primary structure of the DM-20 protein of central nervous system myelin. Proc. Natl. Acad. Sci. USA *84*, 5665–5669.

Norton, W.T. (1974). Isolation of myelin from nerve tissue. In *Methods in Enzymology*, Volume 31, S. Fleischer, and L. Packer, eds. (New York: Academic Press).

Pfeiffer, S.E., Warrington, A., and Bansal, R. (1993). The oligodendrocyte and its many cellular processes. Trends Cell Biol. *3*, 191–197.

Popot, J., Pham Dinh, D., and Dautigny, A. (1991). Major myelin proteolipid: the 4-alpha-helix topology. J. Membr. Biol. *120*, 233–246.

Raine, C.S. (1984). Morphology of myelin and myelination. In *Myelin*, 2nd edition, P. Morell, ed. (New York: Plenum Press), pp. 1–50.

Raskind, W.H., Williams, C.A., Hudson, L.D., and Bird, T.D. (1991). Complete deletion of the proteolipid protein gene (PLP) in a family with X-linked Pelizaeus-Merzbacher disease. Am. J. Hum. Genet. *49*, 1355–1360.

Readhead, C., Popko, B., Takahashi, N., Shine, H.D., Saavedra, R.A., Sidman, R.L., and Hood, L. (1987). Expression of a myelin basic protein gene in transgenic shiverer mice: correction of the dysmyelinating phenotype. Cell *48*, 703–712.

Readhead, C., Schneider, A., Griffiths, I., and Nave, K.-A. (1994). Premature arrest of myelin formation in transgenic mice with increased proteolipid protein gene dosage. Neuron *12*, 583–595.

Roach, A., Takahashi, N., Pravtcheva, D., Ruddle, F., and Hood, L. (1985). Chromosomal mapping of mouse myelin basic protein gene and structure and transcription of the partially deleted gene in shiverer mutant mice. Cell *42*, 149–155.

Rosenbluth, J., Stoffel, W., and Schiff, R. (1996). Myelin structure in proteolipid protein (PLP)-null mouse spinal cord. J. Comp. Neurol. *371*, 336–344.

Roussel, G., Neskovic, N.M., Trifilieff, E., Artault, J.C., and Nussbaum, J.C. (1987). Arrest of proteolipid transport through the Golgi apparatus of jimpy brain. J. Neurocytol. *16*, 195–204.

Schneider, A., Montague, P., Griffiths, I., Fanarraga, M., Kennedy, P., Brophy, P., and Nave, K.-A. (1992). Uncoupling of hypomyelination and glial cell death by a mutation in the proteolipid protein gene. Nature *358*, 758–761.

Schneider, A., Readhead, C., Griffiths, I., and Nave, K.A. (1995). Dominant-negative action of the *jimpy* mutation in mice complemented with an autosomal transgene for myelin proteolipid protein. Proc. Natl. Acad. Sci. USA *92*, 4447–4451.

Seitelberger, F., Urbanitz, I., and Nave, K.-A. (1996). Pelizaeus-Merzbacher disease. In *Handbook of Clinical Neurology*, P. J. Vinken, and G. W. Bruyn, eds. (Amsterdam: Elsevier), in press.

Skoff, R.P. (1995) Programmed cell death in the dysmyelinating mutants. Brain Pathol. *5*, 283–288.

Snipes, G.J., and Suter, U. (1995). Molecular basis of common hereditary motor and sensory neuropathies in humans and in mouse models. Brain Pathol. *5*, 233–247.

Snipes, G.J., Suter, U., and Shooter, E. (1993). The genetics of myelin. Curr. Opin. Neurobiol. *3*, 694–702.

Tan, S.-S., Faulkner-Jones, B., Breen, S.J., Walsh, M., Bertram, J.F., and Reese, B.E. (1995). Cell dispersion patterns in different cortical regions studied with an X-inactivated transgenic marker. Development *121* 1029–1039.

Timsit, S., Martinez, S., Allinquant, B., Peyron, F., Puelles, L., and Zalc, B. (1995). Oligodendrocytes originate in a restricted zone of the embryonic ventral neural tube defined by DM-20 mRNA expression. J. Neurosci. *15*, 1012–1024.

Tosic, M., Dolivo, M., Domanska-Janik, K., and Matthieu, J.M. (1994). Paralytic tremor (pt): a new allele of the proteolipid protein gene in rabbits. J. Neurochem. *63*, 2210–2216.

Weimbs, T., and Stoffel, W. (1992). Proteolipid protein (PLP) of CNS myelin: positions of free, disulfide-bonded, and fatty acid thioester-linked cysteine residues and implications for the membrane topology of PLP. Biochemistry *31*, 12289–12296.

Yan, Y., Lagenaur, C., and Narayanan, V. (1993). Molecular cloning of M6: identification of a PLP/DM-20 gene family. Neuron *11*, 423–431.

Yanagisawa, K., and Quarles, R.H. (1986). Jimpy mice: quantitation of myelin-associated glycoprotein and other proteins. J. Neurochem. *47*, 322–325.

Yoshida, M., and Colman, D.R. (1996). Parallel evolution and coexpression of the proteolipid proteins and protein zero in vertebrate myelin. Neuron *16*, 1115–1126.